Probing ultrafast internal conversion of o-xylene via femtosecond time-resolved photoelectron imaging

Yuzhu Liu,[1] Bifeng Tang,[2] Huan Shen,[1] Song Zhang,[1] and Bing Zhang[1]*

[1]State Key Laboratory of Magnetic Resonance and Atomic and Molecular Physics, Wuhan Institute of Physics and Mathematics, Chinese Academy of Sciences-Wuhan National Laboratory for Optoelectronics, Wuhan, Hubei 430071, PR China Graduate School of the Chinese Academy of Sciences, Beijing 100049, PR China
[2]Department of physics, Xiaogan University, Xiaogan City, Hubei 432000, PR China
**bzhang@wipm.ac.cn*

Abstract: The dynamics of excited states in o-xylene molecules has been studied by femtosecond time-resolved photoelectron imaging coupled with time-resolved mass spectroscopy. The ultrafast internal conversion from the S_2 state to the vibrationally hot S_1 state on timescale of 60 fs is observed on real time. The secondarily populated high vibronic S_1 state deactivates further to the S_0 state on timescale of 9.85 ps. Interestingly, the lifetime of the low vibronic S_1 state is much longer, extrapolated to ~12.7 ns. The great differences of lifetime of different vibronic S_1 state are due to their different radiationless dynamics.

OCIS codes: (020.0020) Atomic and molecular physics; (320.7150) Ultrafast spectroscopy.

References and links

1. I. V. Hertel, and W. Radloff, "Ultrafast dynamics in isolated molecules and molecular clusters," Rep. Prog. Phys. **69**(6), 1897–2003 (2006).
2. A. H. Zewail, "Laser Femtochemistry," Science **242**(4886), 1645–1653 (1988).
3. A. H. Zewail, "Femtochemistry: Atomic-Scale Dynamics of the Chemical Bond Using Ultrafast Lasers," Angew. Chem. Int. Ed. **39**(15), 2586–2631 (2000).
4. A. Stolow, "Femtosecond time-resolved photoelectron spectroscopy of polyatomic molecules," Annu. Rev. Phys. Chem. **54**(1), 89–119 (2003).
5. T. Suzuki, "Femtosecond time-resolved photoelectron imaging," Annu. Rev. Phys. Chem. **57**(1), 555–592 (2006).
6. D. H. Paik, I.-R. Lee, D.-S. Yang, J. S. Baskin, and A. H. Zewail, "Electrons in finite-sized water cavities: hydration dynamics observed in real time," Science **306**(5696), 672–675 (2004).
7. N. K. Schwalb, and F. Temps, "Ultrafast electronic relaxation in guanosine is promoted by hydrogen bonding with cytidine," J. Am. Chem. Soc. **129**(30), 9272–9273 (2007).
8. A. Stolow, A. E. Bragg, and D. M. Neumark, "Femtosecond time-resolved photoelectron spectroscopy," Chem. Rev. **104**(4), 1719–1758 (2004).
9. W. M. Kwok, C. Ma, and D. L. Phillips, "A doorway state leads to photostability or triplet photodamage in thymine DNA," J. Am. Chem. Soc. **130**(15), 5131–5139 (2008).
10. C. Daniel, J. Full, L. González, C. Lupulescu, J. Manz, A. Merli, Š. Vajda, and L. Wöste, "Deciphering the reaction dynamics underlying optimal control laser fields," Science **299**(5606), 536–539 (2003).
11. A. M. Rijs, M. H. M. Janssen, E. T. Chrysostom, and C. C. Hayden, "Femtosecond coincidence imaging of multichannel multiphoton dynamics," Phys. Rev. Lett. **92**(12), 123002 (2004).
12. P. Kukura, D. W. McCamant, S. Yoon, D. B. Wandschneider, and R. A. Mathies, "Structural observation of the primary isomerization in vision with femtosecond-stimulated Raman," Science **310**(5750), 1006–1009 (2005).
13. M. Lenner, and C. Spielmann, "Femtosecond time-resolved saturation dynamics of BDN-doped polycarbonate," Opt. Express **14**(5), 1850–1855 (2006).
14. A. Stolow, V. Blanchet, M. Z. Zgierski, and T. Seideman, "Discerning vibronicmolecular dynamics using time-resolved photoelectron spectroscopy," Nature **401**(6748), 52–54 (1999).
15. M. Oku, Y. Hou, X. Xing, B. Reed, H. Xu, C. Chang, C. Y. Ng, K. Nishizawa, K. Ohshimo, and T. Suzuki, "3s Rydberg and cationic States of pyrazine studied by photoelectron spectroscopy," J. Phys. Chem. A **112**(11), 2293–2310 (2008).
16. W. Domcke, and G. Stock, "Theory of ultrafast nonadiabatic excited-state processes and their spectroscopic detection in real time," Adv. Chem. Phys. **100**, 1–169 (1997).
17. J. H. Callomon, J. E. Parkin, and R. Lopez-Delgado, "Non-radiative relaxation of the excited Ã 1B2u state of benzene," Chem. Phys. Lett. **13**(2), 125–131 (1972).

#122474 - $15.00 USD Received 8 Jan 2010; revised 11 Feb 2010; accepted 12 Feb 2010; published 8 Mar 2010

18. A. E. W. Knight, C. S. Parmenter, and M. W. Schuyler, "An extended view of the benzene 260 nm transition via single vibronic level fluorescence. I. General aspects of benzene single vibronic level fluorescence," J. Am. Chem. Soc. **97**(8), 1993–2005 (1975).
19. A. E. W. Knight, C. S. Parmenter, and M. W. Schuyler, "An extended view of the benzene 260 nm transition via single vibronic level fluorescence. II. Single vibronic level fluorescence as a probe in the assignment of the absorption spectrum," J. Am. Chem. Soc. **97**(8), 2005–2013 (1975).
20. P. Farmanara, V. Stert, W. Radloff, and I. V. Hertel, "Ultrafast internal conversion in highly excited toluene monomers and dimmers," J. Phys. Chem. A **105**(23), 5613–5617 (2001).
21. Y. Wang, S. Zhang, Z. Wei, Q. Zheng, and B. Zhang, "Br(2Pj) atom formation dynamics in ultraviolet photodissociation of tert-butyl bromide and iso-butyl bromide," J. Chem. Phys. **125**(18), 184307 (2006).
22. Y. Liu, Q. Zheng, Y. Zhang, R. Zhang, Y. Wang, and B. Zhang, "Photolysis of 1-C4H9I and 2-C4H9I at 266 nm: direct observation of the effect of branching on the photodissociation mechanism," ChemPhysChem **10**(5), 830–834 (2009).
23. Z. Wei, F. Zhang, Y. Wang, and B. Zhang, "Predissociation Dynamics of B State of Methyl Iodide with Femtosecond Pump-probe Technique," Chin. J. Chem. Phys. **20**(4), 419–424 (2007).
24. V. Dribinski, A. Ossadtchi, V. A. Mandelshtam, and H. Reisler, "Reconstruction of Abel-transformable images: The Gaussian basis-set expansion Abel transform method," Rev. Sci. Instrum. **73**(7), 2634–2642 (2002).
25. L. Wang, H. Kohguchi, and T. Suzuki, "Femtosecond time-resolved photoelectron imaging," Faraday Discuss. **113**, 37–46 (1999).
26. W. Radloff, V. Stert, Th. Freudenberg, I. V. Hertel, C. Jouvet, C. Dedonder-Lardeux, and D. Solgadi, "Inernal conversion in highly excited benzene and benzene dimmer: femtosecond time-resolved photoelectron spectroscpy," Chem. Phys. Lett. **281**(1-3), 20–26 (1997).
27. C. N. Yang, "On the angular distribution in nuclear reactions and coincidence measurements," Phys. Rev. **74**(7), 764–772 (1948).
28. T. Droz, S. Leutwyler, M. Mandziuk, and Z. Bačić, "Intermolecular vibrations of o-xylene·Ar in the S0 and S1 states: Experiment and quantum three dimensional calculations," J. Chem. Phys. **101**(8), 6412–6423 (1994).
29. T. A. Stephenson, and S. A. Rice, "Vibrational state dependence of radiationless processes in 1B2u benzene," J. Chem. Phys. **81**(3), 1073–1082 (1984).
30. W. A. Noyes, Jr., "W. A. Mulac, D. A. Harter, "Some aspects of the photochemistry of benzene," J. Chem. Phys. **44**(5), 2100–2106 (1966).
31. P. T. Whiteside, A. K. King, and K. L. Reid, "Photoelectron spectroscopy of S1 toluene: I. Photoionization propensities of selected vibrational levels in S1 toluene," J. Chem. Phys. **123**(20), 204316 (2005).
32. P. T. Whiteside, A. K. King, J. A. Davies, K. L. Reid, M. Towrie, and P. Matousek, "Photoelectron spectroscopy of S1 toluene: II. Intramolecular dynamics of selected vibrational levels in S1 toluene studied by nanosecond and picosecond time-resolved photoelectron spectroscopies," J. Chem. Phys. **123**(20), 204317 (2005).
33. K. G. Spears, and S. A. Rice, "Study of the Lifetimes of Individual Vibronic States of the Isolated Benzene Molecule," J. Chem. Phys. **55**(12), 5561–5581 (1971).
34. L. Wunsch, H. J. Neusser, and E. W. Schlag, "Two-photon absorption in the collisionless gas phase: lifetimes of new vibrational levels in benzene," Chem. Phys. Lett. **32**(2), 210–215 (1975).
35. M. Clara, Th. Hellerer, and H. J. Neusser, "Fast decay of high vibronic S1 state in gas-phase benzene," Appl. Phys. B **71**, 431–437 (2000).
36. E. Riedle, H. J. Neusser, and E. W. Schlag, "Sub-Doppler high-resolution spectra of benzene: anomalous results in the "channel three" region," J. Phys. Chem. **86**(25), 4847–4850 (1982).
37. A. L. Sobolewski, C. Woywod, and W. Domcke, "Ab initio investigation of potential-energy surfaces involved in the photophysics of benzene and pyrazine," J. Chem. Phys. **98**(7), 5627–5641 (1993).
38. D. Bryce-Smith, and H. C. Longuet-Higgins, "Photochemical transformation of the benzene ring," Chem. Commun. **17**(17), 593 (1966).
39. C. E. Otis, J. L. Knee, and P. M. Johnson, "Nonradiative processes in the channel three region of the S1 state of ultracold benzene," J. Phys. Chem. **87**(12), 2232–2239 (1983).

1. Introduction

To understand the nature of inter- and intra-molecular dynamics in detail, to visualize the making and breaking of molecular bonds and to follow in real time the flow of energy and charge within molecular systems, to 'see' the geometrical rearrangements and chemical reactions after energy deposition, have long been dreams of physical chemists and chemical physicists [1]. Only with the advent of ultrafast laser pulses have these dreams become true. The initiation and subsequent control or exploration study of chemical transformations in real time using ultrashort laser pulses is the aim of femtochemistry [2,3]. The real-time investigation of the ultrafast dynamics of molecules in gas and condensed phases has attracted a great deal of attention over the last two decades [4–7]. A significant number of studies have dealt with time-resolved molecular dynamics in systems of increasing complexity [8–15]. However, some basic issues of the real time dynamics are still elusive. New insight into the detailed mechanisms of some simple systems can be obtained by the combination of femtosecond laser systems and detection techniques.

#122474 - $15.00 USD Received 8 Jan 2010; revised 11 Feb 2010; accepted 12 Feb 2010; published 8 Mar 2010

For the detailed study of chemical transformation dynamics in real time, time-resolved photoelectron imaging (TRPEI) has proven to be a powerful technique [5]. TRPEI measures the photoionization differential cross section, i.e. the energy resolved within the probe bandwidth. It thus provides both the energy and the angular distribution of the photoelectrons as well as their correlation as a function of time. It allows for the study of electronic relaxation dynamics in isolated molecules, as well as the study of sequential ultrafast electronic processes in both optically bright and dark states.

Ultrafast electronic relaxation processes [16] play a central role in photochemistry and photobiology, internal conversion (IC) induced by electronic nonadiabaticity and intersystem crossing (ISC) induced by spin-orbit coupling being the two major nonradiative pathways. In polyatomic molecules excited to higher electronic states, internal conversion to vibronic levels of lower electronic states is one of the dominant mechanisms for deactivation. As the prototypical aromatic molecule and the essential structure of numerous biologically important compounds in nature, isolated benzene molecules have been the subject of a great number of investigations. However, the determination of the chemical properties and structure of benzene posted a challenge to scientists for decades. It is well-known that benzene exhibits a sharp, apparently anomalous, fluorescence decrease approximately 3000 cm^{-1} above the origin of the S_1 state ($^1B_{2u}$) for which no satisfying explanation has appeared. This nonradiative channel has come to be known as 'channel three'. It was first observed by Callomon et al. from the diffuseness of the vibronic bands [17]. Consistent with the highly reduced excited state lifetime, they observed only diffuse vibronic bands in the measured spectra. Since they thought that none of the standard processes (IC, ISC or IVR) were responsible, this unknown phenomenon was named 'channel three', and remained mysterious for a long time [18,19].

In the present paper, we report a study on the internal conversion processes in o-xylene as an example of a system with strongly reduced symmetry. The nondegeneracy of states in this benzene derivative leads to a higher density of the vibrational levels and to a reduction of symmetry-forbidden interactions [20]. Hence, higher coupling rates for nonadiabatic transitions are expected. Time-resolved photoelectron imaging and time-resolved mass spectroscopy are used. The internal conversion processes of excited S_2 state excited by two-photon absorption at 400 nm have been directly observed on real-time. The low vibronic S_1 state excited by a pump pulse at 267 nm is also investigated. Finally, The dynamics processes of high vibronic and low vibronic S_1 state are analyzed and compared to get more details about 'channel three' effect.

2. Experiment

The time-resolved photoelectron imaging setup used in this study is similar in spirit to our ion velocity imaging system, which has been described elsewhere [21,22]. The key modification was made by adding a multilayer μ-metal shielding to avoid disturbance of the stray field when collecting the photoelectrons.

The details of our femtosencond laser system have been described elsewhere [23]. Briefly, the seed beam was generated by a commercial Ti:sapphire oscillator pumped by a CW second harmonic of an Nd:YVO_4 laser, and then amplified by an Nd:YLF pumped regenerative amplifier to generate a 1 kHz pulse train centered at 800 nm of 45 fs pulse width with maximum energy of 1 mJ/pulse. The second harmonic pulse (400 nm) was generated in a 0.5 mm thick BBO crystal, and the third harmonic pulse (267 nm) was generated in a 0.2 mm thick BBO crystal by sum frequency mixing of the second harmonic and the fundamental. The pump and probe beams with vertical polarization were merged by a dichroic mirror and directed into the molecular beam chamber. The time delay between the pump and probe pulses were accurately monitored by a computer-controlled linear translation stage (PI, M-126.CG1).

The liquid sample (o-xylene, 99.9% purity), 5% seeded in helium buffer gas at a background pressure of 2 atm, was expanded through a pulsed valve to generate a pulsed

#122474 - $15.00 USD Received 8 Jan 2010; revised 11 Feb 2010; accepted 12 Feb 2010; published 8 Mar 2010

molecular beam. The beam was skimmed and introduced into the ionization chamber where it was intersected perpendicularly by the laser beam.

3. Results

The position of the S_2 state of o-xylene is estimated to be at 5.63 eV from the absorption spectrum. Two-photon absorption at 400 nm is used to populate the S_2 state of o-xylene. The polarizations of both the pump laser (400 nm) and the probe laser (800 nm) are vertical, and are perpendicular to the molecular beam. The mass spectra of o-xylene are obtained when the pump and probe beams are temporally overlapped. They have only two peaks corresponding to $C_6H_4(CH_3)_2^+$ parent ions and $C_6H_4CH_3^+$ ions, respectively. The area ratio of $C_6H_4(CH_3)_2^+$ and $C_6H_4CH_3^+$ is 12:1. Moreover, it is believed that most of the $C_6H_4CH_3^+$ ions are from the dissociation of $C_6H_4(CH_3)_2^+$ parent ions for the time-dependent ion signals of $C_6H_4CH_3^+$ have the similar trend as parent ions. Therefore, the contribution to the total photoelectron signal from the generation of $C_6H_4CH_3^+$ ions can be neglected.

Figure 1 shows the time-resolved total ion signal of the parent ion formed after two-photon excitation of the S_2 state at 400 nm as a function of the pump-probe delay. The decay profiles are fitted with the sum of two exponentials with lifetimes of 60 fs and 9.85 ps convoluted with a Gaussian describes the instrument response function. The fast one (τ_1 = 60 fs) reflects the excitation and decay of the initially excited S_2 state. The dynamics of those decays will be discussed later by energy analysis of the corresponding photoelectrons released from the probe laser pulse.

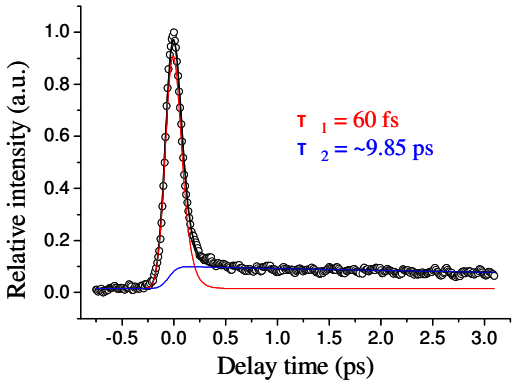

Fig. 1. Time-resolved total ion signals of parent ion as a function of delay time between the pump pulse at 400 nm and the probe pulse at 800 nm. The circles are the experimental results, and solid lines are the fitting results.

The photoelectrons generated by pump-probe photoinization are projected onto a two-dimensional (2D) position-sensitive detector. Photoelectron images are acquired as a function of the pump–probe time delay. Figure 2 shows reconstructed photoelectron images corresponding to such a sequence, inverted by the basis-set expansion method (BASEX) [24]. The BASEX-inverted photoelectron images represent a section of the 3D photoelectron scattering distribution. The signals originating from the different electronic states are generally well resolved in the images. Three well-resolved concentric bands appear in the observed images as the delay time changes. The bands with different radii stand for photoelectrons with different kinetic energy components. The corresponding photoelectron kinetic energy distributions of these images are shown in Fig. 3. The arrows indicate the photoelectron energy (0.74 eV and 2.29 eV) that are expected for ionization to the zero vibrational level of the cation indicated by D_0 and D_0', by two-photon and three-photon absorption of probe pulse. The three bands centered at 0.30, 0.48 and 1.64 eV are assigned as the first, second, and third bands.

#122474 - $15.00 USD Received 8 Jan 2010; revised 11 Feb 2010; accepted 12 Feb 2010; published 8 Mar 2010

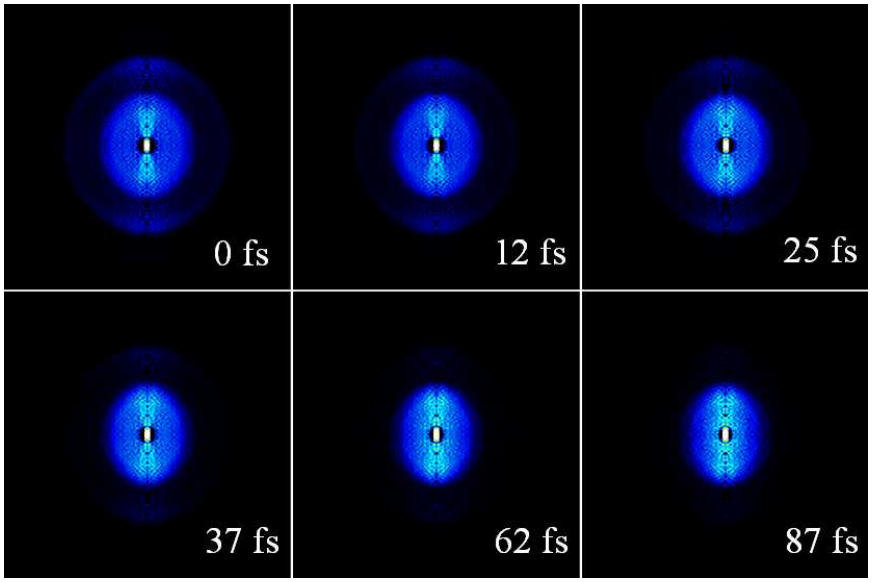

Fig. 2. A series of time-resolved BASEX-inverted photoelectron images of o-xylene observed using a pump laser wavelength of 400 nm and a probe wavelength of 800 nm. The linear polarizations of the pump and probe lasers are aligned vertical in the plane of the figure.

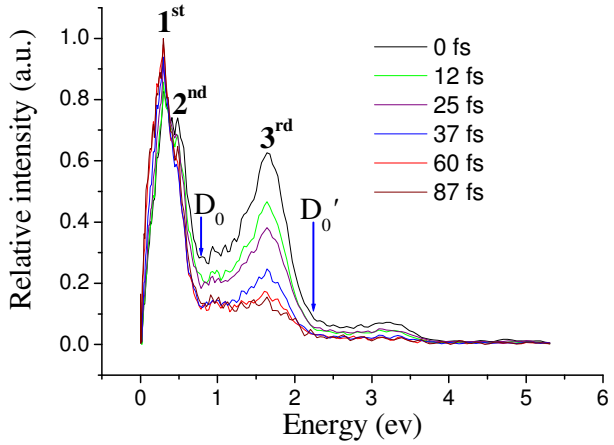

Fig. 3. Photoelectron kinetic energy distributions extracted from the images of Fig. 2. The arrows indicate the photoelectron energy (0.74 eV and 2.29 eV) expected for ionization to the zero vibrational level of the cation indicated by D_0 and D_0', by two-photon and three-photon absorption of probe pulse, respectively.

The experimental PKE (photoelectron kinetic energy) distributions are characterized by a rapid decay of electrons from the second and third bands, and soft growth of the electrons from the first band. Figure 4 shows the time evolution of the total electron signals, which consists of a different biexponential decay behavior, same as the evolution of total ion signals. By masking the phosphor screen and observing the image of the third band with the photomultiplier tube [25], the time evolution of the third band can be measured, which is also shown in Fig. 4. It consists of only one ultrafast component, with the similar decay rate as the S_2 state obtained from the time-resolved ion signals before. Thus, the third band should be due to ionization of the populated S_2 state. The first and second bands overlap too much to be able to measure, the time evolution of the electron signals from these bands cannot be measured

#122474 - $15.00 USD Received 8 Jan 2010; revised 11 Feb 2010; accepted 12 Feb 2010; published 8 Mar 2010

accurately by masking the phosphor screen. As shown in Fig. 3 or Fig. 5, the second band decays in the same manner as the third one, so it should also be from the S_2 state by absorption of photons from the probe pulse. Moreover, the intensity of the signal of the third band depends on the power of the probe pulse. The intensity of the third band decreases when the energy of the probe pulse deceases from 28 uJ to 14 uJ. As expected, the intensity of the second band increase when the ones of the third band decrease, for they are from the same state and compete with each other. The probe pulse (800 nm) ionizes the excited species by two-photon or three-photon absorption to a final excess energy in the ion (or rather the emitted electrons) of $D_0 = 0.74$ eV or $D_0' = 2.29$ eV above the IE (8.56 eV). Therefore, it is obvious that the second and third bands center at 0.48 and 1.64 eV are due to ionization of the populated S_2 state by two-photon and three-photon absorption of probe pulse, respectively. The second and third bands decay rapidly with increasing time, revealing that the populated S_2 state undergoes a very rapid internal conversion into vibrationally excited lower states. Its order of magnitude has already been estimated to be 60 fs from the time dependence of the ion signal. The first band grows slightly with increasing delay time within the time window shown in Fig. 3. Its appearance is due to population of the S_1 state by internal conversion from the S_2 state. It arises from photoionization of the S_1 state by three-photon absorption of probe pulse for higher vibrational levels since electronic excitation energy of S_2 state is converted into vibrational excitation energy of S_1 state. All the ionization mechanism and IC dynamics analyzed here are shown in Fig. 6.

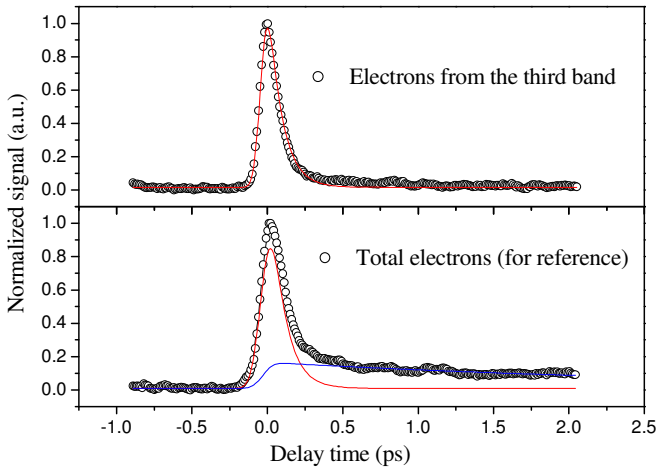

Fig. 4. Time evolution of photoelectron signals only from the third band and total photoelectron signals (for reference) with the pump pulse at 400 nm and the probe pulse at 800 nm.

#122474 - $15.00 USD Received 8 Jan 2010; revised 11 Feb 2010; accepted 12 Feb 2010; published 8 Mar 2010

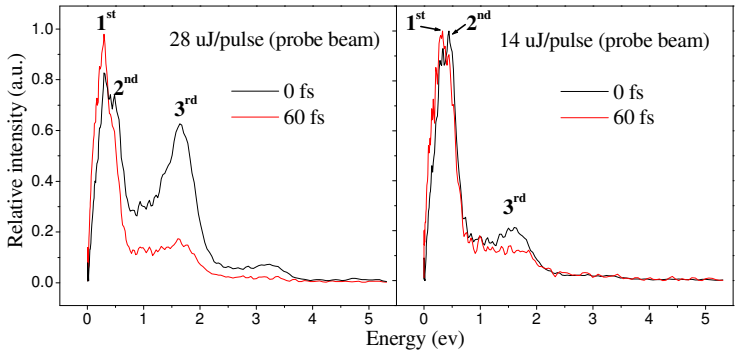

Fig. 5. Time-resolved PKE distributions with two energies of the probe pulse (800 nm) and the same energy of the pump pulse (400 nm).

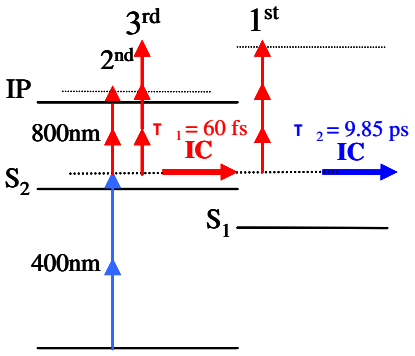

Fig. 6. Energy excitation scheme of the ground, excited and ionic states of o-xylene. The pump laser (400 nm) prepares the S_2 state. Due to ultrafast internal conversion, this state converts to the lower-lying state S_1 with higher vibrational energy. Here, 1st, 2nd and 3rd are corresponding to the first, second and third bands marked on Fig. 3.

The results of PKE distributions contain more information than the overall internal conversion time. It can be seen from Fig. 3 or Fig. 5 that the relative intensities of the second and third photoelectron bands corresponding to S_2 state decay very strongly while one of the first photoelectron band corresponding to S_1 state grows very slightly. This can be explained by proposing that the decay process of the populated S_2 state is attributed to simultaneous internal conversion from the S_2 state to higher vibrational levels of S_1 and S_0 state with the later process being the dominant mechanism. Highly excited benzene and toluene have been studied by W. Radloff et al. and their results show that the S_2 to S_1 transition occurs only with a small branching ratio of 1% for benzene [26] and 30% for toluene [20] respectively. The internal conversion of the S_2 state leads mainly to the highly excited S_0 state, the population of which cannot be observed in our pump-probe experiments since the corresponding Franck-Condon factors are extremely low. It also can be seen clearly in Fig. 5 that there is vibrational structure in the photoelectron spectra. This structure yields information about the state-to-state vibrational dynamics which promotes and tunes the electronic population transfer, and the ensuing intramolecular vibrational energy redistribution in the hot molecule which occurs on the potential surface of excited states [14].

In our experimental configuration with the linear and parallel polarization of the pump and probe laser beams, the laboratory frame photoelectron angular distributions (PADs) resulting from ionization can be expanded as [27]

#122474 - $15.00 USD Received 8 Jan 2010; revised 11 Feb 2010; accepted 12 Feb 2010; published 8 Mar 2010

$$I(\theta;t) = \sigma(t)[1 + \beta_2(t)P_2(\cos\theta) + \beta_4(t)P_4(\cos\theta) + \beta_6(t)P_6(\cos\theta)], \quad (1)$$

where $\sigma(t)$ is the integral cross section, $\beta_L(t)$ are the anisotropy parameters, $P_L(cos\theta)$ are Legendre polynomials, and θ the angle between the laser polarization direction and the direction of the ejected electron k-vector. Time-resolved PADs are extracted from the time-resolved reconstructed images. Three anisotropy coefficients β_2, β_4 and β_6 are obtained for different photoelectron bands at different time delays, respectively. No significant changes of PADs of the third band (with distributions of PKE of 0.76-2.29 eV) at different time delays are observed, which verifies no existence of rotational coherence in our experiment. The first and second bands overlap too much, and it is difficult to accurately get their PADs. PADs with distributions of PKE of 0-0.74 eV, which contains the first and second bands, are obtained. And those distributions and fitted results are displayed as polar plots in Fig. 7. PADs changes gradually from delay time of 0 fs (β_2 = 0.556) to 87 fs (β_2 = 1.029). Moreover, no significant changes of PADs of the third band (with distributions of PKE of 0.76-2.29 eV) at different time delays are observed, which verifies no existence of rotational coherence in our experiment. Therefore, the time evolution of PADs with distributions of PKE of 0-0.74 eV reveals ultrafast IC from S_2 state to S_1 state, which is consistent with the discussion by time-resolved PKE distributions before.

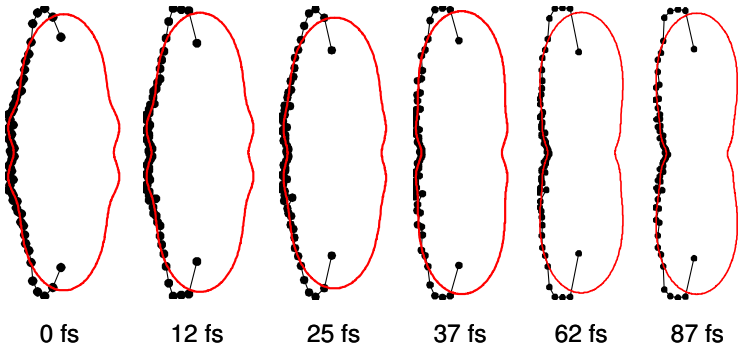

Fig. 7. Polar plots of PADs with distributions of PKE of 0-0.74 eV observed for different time delays of pump (400 nm) and probe pulse (800 nm). The linear polarizations of the pump and probe lasers are aligned vertical in the plane of the figure.

The energy levels of the excitation of the o-xylene molecule at an energy of the 6.21 eV pump photons will lead to a vibrational energy of 1.58 eV in the S_1 state after conversion from the S_2 state. The lifetime of this vibrationally hot S_1 state from the time dependence of the obtained is about 9.85 ps. However, the deactivation mechanism for the S_1 state is still unknown from the above work.

To obtain further information about the S_1 state, a femtosecond pump pulse at 267 nm (4.65 eV) is used to prepare the low vibronic levels of the S_1 excited state, only slightly above the electronic origin (4.63 eV) [28]. These excited vibronic levels of the S_1 o-xylene molecules are then ionized by two-photon absorption at 400 nm. This results in an excess energy above the IE of up to 2.30 eV. Figure 8 shows signals of parent ion as a function of the pump-probe delay in this (1 + 2′)-REMPI experiment. The power of pump and probe pulses are modulated to make sure that no any enhancement of signals is observed in negative time-delay direction. The mass spectra of o-xylene obtained at the temporal overlap of the pump and the probe light have only two peaks corresponding to $C_6H_4(CH_3)_2^+$ parent ions and $C_6H_4CH_3^+$ ions, respectively. The ratio of the parent and daughter ion signals is 9:1. Same as discussion before, the generation of $C_6H_4CH_3^+$ ions has no contribution to the total photoelectron signal.

#122474 - $15.00 USD Received 8 Jan 2010; revised 11 Feb 2010; accepted 12 Feb 2010; published 8 Mar 2010

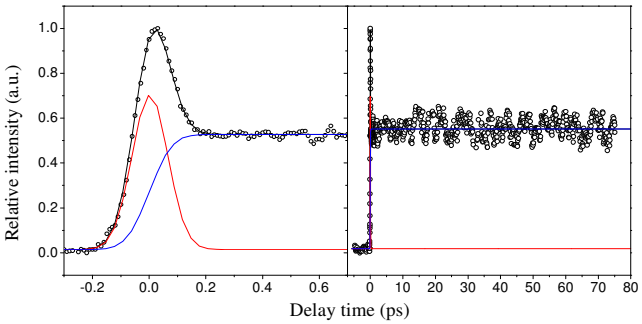

Fig. 8. Time-resolved signals of parent ion as a function of the pump-probe delay observed using a pump laser wavelength of 267 nm and a probe wavelength of 400 nm. The circles are the experimental results, and solid lines are the results of a fit < 50 fs for the initial delay and ~12.7 ns for the second delay.

As shown in Fig. 8, these transients exhibit an extremely fast initial decay around the zero delay time followed by a much slower temporal feature. The fitting results for these transients reveal a decay time τ_1 for an extremely fast initial decay that is less than 50 fs, which is faster than the time resolution of the experiment. The second decay time τ_2 for the much slower one is too long, far above the upper limit of the time delay stage (167 ps). Therefore it is not determined accurately. Nevertheless, the extrapolated state lifetime is about ~12.7 ns.

More detailed information about the dynamics can be learned from the snapshots of electron scattering distributions taken at different time delays as shown in Fig. 9. It seems that no significant changes can be seen in these snapshots. To examine this more quantitatively, the photoelectron kinetic energy distributions extracted from the images are presented in Fig. 10. No ultrafast nonradiative electronic relaxation process is observed from the time-resolved PKE distributions. What is more, the first component can be fitted well by a Gaussian function with a width of 126 fs for the cross-correlation for the pulses of 400 nm and 267 nm. Therefore, τ_1 represent a coherent "artifact", which shows up due to a cross correlation between the pump and probe laser beams at zero delay time. Cross correlated ion signals can be approved or ruled out by varying the pump and probe powers, because of their strong power dependences. The impact of cross correlated ion signals cannot be neglected in REMPI experiment with weak enhancement, like the low vibronic S_1 state investigated here.

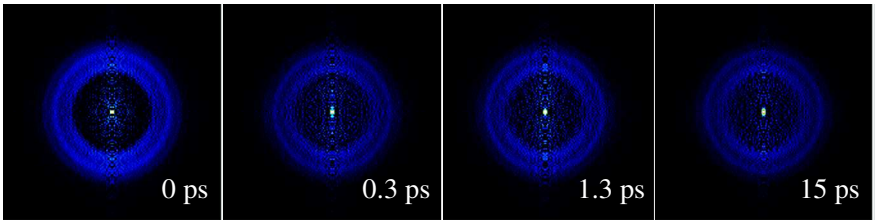

Fig. 9. A series of time-resolved BASEX -inverted photoelectron images of o-xylene observed using a pump laser wavelength of 267 nm and a probe wavelength of 400 nm. The linear polarizations of the pump and probe lasers are aligned vertical in the plane of the figure.

#122474 - $15.00 USD Received 8 Jan 2010; revised 11 Feb 2010; accepted 12 Feb 2010; published 8 Mar 2010

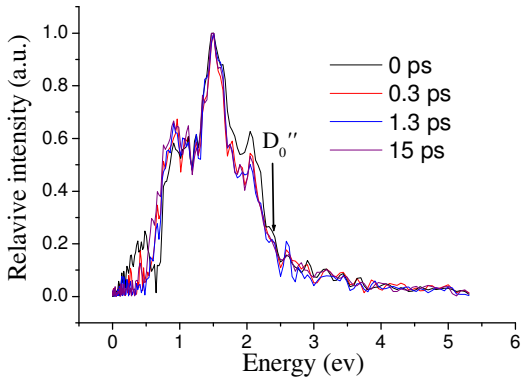

Fig. 10. Photoelectron kinetic energy distributions extracted from the images of Fig. 9. The arrow indicate the photoelectron energy (D_0'' = 2.30 eV) expected for ionization to the zero vibrational level.

For there is no ultrafast nonradiative electronic relaxation process observed, the second component with timescale of ~12.7 ns reflects the population of the low vibronic S_1 state. It is in agreement with the previous studies for similar molecules of benzene and toluene. Benzene has a long lifetime of 106 ns at its S_1 origin [29]. At low excess energies in S_1 state of benzene, the fluorescence quantum yield is about 0.2 [30] and it was concluded that intersystem crossing to the $^3B_{1u}$ triplet state is responsible for the nonradiative deactivation. S_1 toluene has been investigated by nano- and picosecond time-resolved photoelectron spectroscopy [31,32]. The excitation of different vibrational modes up to an excess energy of 1200 cm^{-1} revealed nonradiative deactivation in several hundred ps to several ns from all of the prepared states. Intersystem crossing to the triplet state was observed at pump-probe delay times of > 30 ns. Therefore, it is reasonable to attribute the slow nonradiative deactivation of the low vibronic S_1 state of o-xylene with timescale of ~12.7 ns to a slow intersystem crossing process.

It is interesting to note that the lifetime for the low vibronic S_1 state discussed here increases by three orders of magnitude, compared with high vibronic S_1 state discussed before. The lifetime of the high vibronic S_1 state with excess energy of 1.58 eV, populated by inernal conversion from S_2 state by two-photon absorption of pump pulse at 400 nm, is 9.85ps. While for low vibronic S_1 states with excess energy of 0.02 eV, excited by a pump pulse at 267 nm, the lifetime is much longer, about ~12.7 ns. The great differences in the dynamics in different vibronic levels of the S_1 state are surprising. Similar phenomenon called 'channel three' has also been observed in benzene. At low excess energies in S_1, the lifetime of vibrational levels is in the range of 60 to 120 ns [33,34], and no ultrafast processes is observed [35]. This quite normal behavior is observed for vibratinal levels up to an excess energy of 3000 cm^{-1}. Then a sudden increase of the decay rate occurs, increasing by up to 1000 times. It is known that higher vibrational levels of the S_1 electronic state as well as S_2 state levels are deactivated very fast by internal conversion [36,37]. This behavior is explained by a conical intersection of the S_1 and S_0 potential-energy surfaces [37,38]. Otis et al. have also studied nonradiative processes in the 'channel three' region of the S_1 state of ultracold benzene [39]. At vibrational energies greater than 3000 cm^{-1}, the quantum yield for intersystem crossing decreases markedly relative to the lower lying levels. Their data suggests that the major channel for S_1 relaxation is internal conversion. In our experiment, the 'channel three' effect is also observed for o-xylene. The S_1 state of o-xylene populated above the 'channel three' region via internal conversion from S_2 state, the conical intersection of the S_1 and S_0 potential-energy surfaces is accessible, and this reduces the S_1 lifetime from nanosecond to picosecond.

#122474 - $15.00 USD Received 8 Jan 2010; revised 11 Feb 2010; accepted 12 Feb 2010; published 8 Mar 2010

4. Conclusion

We have used femtosecond time-resolved pump–probe photoelectron imaging to observe ultrafast processes arising from the optically excited states of o-xylene on real time. By two-photon absorption at 400 nm, the S_2 state is excited and the lifetime of internal conversion to lower excited states is determined to be 60 fs according to the decay of the ion signals. A rapid shift of electrons from S_2 state to S_1 state is observed by time-resolved PKE distributions, which show internal conversion processes in real time. The internal conversion of the S_2 state to the highly excited S_0 state cannot be observed directly, but it is found to be an important channel.

The 'channel three' effect is observed in the S_1 state of o-xylene. The lifetime of the S_1 state depends strongly on the vibronic excess energy. The great differences of lifetime of different vibronic S_1 state are attributed to their different radiationless dynamics. The high vibronic S_1 state populated above the 'channel three' region via internal conversion from S_2 state deactivates further through a conical intersection to the S_0 state on a time scale of 9.85ps. For low vibronic S_1 state excited by pump pulse at 267 nm, no ultrafast nonradiative electronic relaxation process is observed. The lifetime is much longer, extrapolated to be ~12.7 ns, which is due to a slow intersystem crossing process.

Acknowledgments

This work was supported by the National Natural Science Foundation of China under Grant nos. 10704083 and 20673140.

#122474 - $15.00 USD Received 8 Jan 2010; revised 11 Feb 2010; accepted 12 Feb 2010; published 8 Mar 2010